Journal of Computational Physics 228 (2009) 2643–2659

Contents lists available at ScienceDirect

Journal of Computational Physics

journal homepage: www.elsevier.com/locate/jcp

Design of piezoelectric actuators using a multiphase level set method of piecewise constants

Zhen Luo [a], Liyong Tong [a,*], Junzhao Luo [b], Peng Wei [c], Michael Yu Wang [c]

[a] School of Aerospace, Mechanical and Mechatronic Engineering, The University of Sydney, Sydney, NSW 2006, Australia
[b] National Engineering Research Center for CAD, Huazhong University of Science and Technology, Wuhan, Hubei 430074, PR China
[c] Department of Mechanical and Automation Engineering, The Chinese University of Hong Kong, Shatin NT, Hong Kong SAR, PR China

ARTICLE INFO

Article history:
Received 19 May 2008
Received in revised form 12 December 2008
Accepted 17 December 2008
Available online 27 December 2008

Keywords:
Shape and topology optimization
Level set methods
Piezoelectric actuators
Compliant mechanisms
Multiple phases

ABSTRACT

This paper presents a multiphase level set method of piecewise constants for shape and topology optimization of multi-material piezoelectric actuators with in-plane motion. First, an indicator function which takes level sets of piecewise constants is used to implicitly represent structural boundaries of the multiple phases in the design domain. Compared with standard level set methods using n scalar functions to represent 2^n phases, each constant value in the present method denotes one material phase and 2^n phases can be represented by 2^n pre-defined constants. Thus, only one indicator function including different constant values is required to identify all structural boundaries between different material phases by making use of its discontinuities. In the context of designing smart actuators with in-plane motions, the optimization problem is defined mathematically as the minimization of a smooth energy functional under some specified constraints. Thus, the design optimization of the smart actuator is transferred into a numerical process by which the constant values of the indicator function are updated via a semi-implicit scheme with additive operator splitting (AOS) algorithm. In such a way, the different material phases are distributed simultaneously in the design domain until both the passive compliant host structure and embedded piezoelectric actuators are optimized. The compliant structure serves as a mechanical amplifier to enlarge the small strain stroke generated by piezoelectric actuators. The major advantage of the present method is to remove numerical difficulties associated with the solution of the Hamilton–Jacobi equations in most conventional level set methods, such as the CFL condition, the regularization procedure to retain a signed distance level set function and the non-differentiability related to the Heaviside and the Delta functions. Two widely studied examples are chosen to demonstrate the effectiveness of the present method.

1. Introduction

Microactuators are now becoming increasingly popular as they offer significant potential in a broad range of engineering applications. Amongst a variety of actuators, piezoelectric material based actuation has been considered as one of the most appealing means due to its favorable characteristics, e.g. high energy densities in nanometer range, fast response time and large loading capacity [15,29]. It is well known that the piezoelectric actuator uses the inverse rather than the direct piezoelectric effect to convert electric energy to mechanical actuation. This research concentrates on the design of piezoelectric

* Corresponding author. Tel.: +61 2 93516949; fax: +61 2 93514841.
E-mail addresses: zluo@aeromech.usyd.edu.au (Z. Luo), ltong@aeromech.usyd.edu.au (L. Tong).

0021-9991/$ - see front matter © 2008 Elsevier Inc. All rights reserved.
doi:10.1016/j.jcp.2008.12.019

actuators capable of generating in-plane motion rather than out-of plane motion. The devices with in-plane motion are more suitable for micro-mechanical systems [1] because of the consideration of the microscale packaging process.

A range of methods have been developed for the design of piezoelectric actuators in the context of smart structures. As noted in [15], a large portion of current research, however, either concentrates on optimal design of host compliant structure with one or more pre-determined actuators [40,11] or concerns with the design of the actuator with given structure [18,42]. It is noted that both design methods impose a limitation on the optimality of the piezoelectric actuation system [15]. Since the performance of a smart actuator is dependent on the coupling between a host structure and its attached piezoelectric actuators [8,10], a more potential way is to simultaneously optimize both piezoelectric actuators (placements, shapes, topologies, etc.) and their host structure (shape and topology) via a numerical process of distributing the elastic material, the piezoelectric material and the void material in the design domain at the same time. Thus, the piezoelectric actuator considered in this work is such a device in which a passive compliant host structure is actuated by embedded piezoelectric elements to generate in-plane motions at specific positions. Since the actuators designed in this way is usually subject to small strain stroke [40], the host structure serves as a compliant mechanical amplifier to enlarge the small stroke produced by piezoelectric materials [19,11,22]. A piezoelectric actuator can therefore be regarded as an electromechanically actuated compliant mechanism [17] capable of accomplishing complex in-plane movements without the use of conventional joints and pins. Such smart actuators are particularly suitable for transmitting nanometer to micrometer displacement in micro-mechanical systems (MEMS) [1]. Hence, this study aims to develop a systematic design method for multiphysics and multi-material smart actuators with in-plane motions using a new shape and topology optimization method.

The goal of topology optimization is to find the optimal distribution of a given amount of material via an iterative numerical process in an extended fixed domain to extremize a specified objective function [14,5]. The field of topology optimization has experienced considerable advance during the past decade with development of different methods, e.g. the homogenization method [4], the SIMP method [55,28,6], the evolutionary structural optimization (ESO) method [53], the level set method including both the standard level set-based methods [37,33,47,2] and the parameterization or equivalent level set methods [3,16,49,26,27,50]. Amongst a variety of possible applications of the topology optimization method, the design of piezoelectric actuators has been very promising [11,8,10,20]. However, most current studies are mainly concerned with single material design and the research on multi-material design is relatively rare. Hence, only a few available publications are on multi-material shape and topology optimization problems, which mostly employ material distribution (Homogenization or SIMP) methods in conjunction with a rule of mixtures to implement multiphase modeling. For instance, Sigmund [39] studied a hybrid power-law interpolation scheme to describe the effective material properties for electrothermomechanical multiphysics actuators, by combining the Hashin–Shtrikman bounds with the standard power-law penalization method. Buehler et al. [8] used the homogenization method to implement the simultaneous design of a given amount of non-piezoelectric and piezoelectric material in the design domain with un-pre-determined sizes and shapes. Carbonari et al. [10] used a SIMP based power-law interpolation scheme to address the placements of the piezoelectric materials and the topology of the flexible structure, but it was reported that the material interpolation model applied suffers from several well-recognized drawbacks [39]. There are still two fundamental issues [48] that are in debate when applying the material distribution method to the multi-material topology optimization: the material interpolation scheme and the ill-posedness of the optimization problem.

There have been several methods for the multiphase motions using level sets [54,12,46,48,23,24]. Vese and Chan [46] proposed a level set multiphase scheme to implement image segmentation using the Mumford and Shah model, which requires $\log n$ level set functions for n segments or phases in the piecewise constant case. Wang and Wang [48] studied a "color" level set model for the shape and topology optimization of multiphase material problems [48] based on the standard level set method [32,36,34], which represents 2^n different material phases using n level set functions. However, this method may lead to some empty regions if the number of the multiple phases is not exactly equal to 2^n, because in this case the total number of the phases is over estimated. The standard level set-based methods suffer from several numerical difficulties related to the implementation of the Hamilton–Jacobi equation [49,26]. Tai et al. [23,24,44] proposed a piecewise constant "level set" method (PCLSM) to identify curves separating regions into different phases in Mumford–Shah image segmentation, which only uses one indicator function taking piecewise constants rather than several level set functions to represent multiple phases. Wei and Wang [50] studied the basic application of the piecewise constant "level set" method [23,24] to structural shape and topology optimization problems, but it is merely concentrated on structural stiffness designs involving one single material. However, the most attractive feature of PCLSM is to represent and identify the boundaries of the multiphase motions [54,35,46].

Therefore, this study presents a shape and topology optimization method for multiphysics and multi-material piezoelectric actuators using PCLSM [23,24,43,44]. An indicator function consisting of several piecewise constants is applied to model different regions in the entire design domain for multi-material smart actuators. Each constant value function involved in the level set function is used to uniquely represent one material phase, and n different phases require n piecewise constant value functions. A minimization functional is defined as a smooth energy term to formulate the optimization problem with the specified constraints. In doing so, the design optimization is converted into a process of renewing all the constant value functions using a semi-implicit AOS algorithm [25,52] to descend the design sensitivity [27], until the shape and topology of both host structure and the locations, shapes and topologies of piezoelectric materials are optimized in the same design domain simultaneously. The major characteristic of PCLSM [24,23] is to remove the connection between the level set functions and re-initializations of the signed distance function, to totally relax the time step limitation imposed by the CFL condition, and

to avoid the non-differentiability related to the Heaviside and Delta functions. It should be noted that the level set function in this study refers to an indicator function including piecewise constant functions [43,44] that is different from the concept in the standard level set method [32,36] which are some Lipschitz continuous functions.

2. Piezoelectric finite element model

The constitutive equations describing the piezoelectric plate are based on the assumption that the total strain in the actuator is the sum of mechanical strain caused by the applied electric voltage. The equations for the linear piezoelectric material under quasi-static models can be written in tensor form as [21,7]:

$$\sigma_{ij} = C_{ijkl}\varepsilon_{kl} - e_{kij}E_k, \tag{1}$$

$$D_i = e_{ikl}\varepsilon_{kl} + \lambda_{ik}E_k, \tag{2}$$

where C_{ijkl}, ε_{kl} and σ_{ij} (for 3D $i,j = 1,2,3$, $k,l = 1,2,3$) represents mechanical elastic tensor, strain and stress tensor, respectively. e_{kij}, λ_{ik}, E_k and D_i are matrices of piezoelectric constant, permittivity constant of mechanical constant strain, electric field and electric displacement, respectively. It should be pointed out that Eq. (1) denotes the direct piezoelectric effect while Eq. (2) shows the converse piezoelectric effect.

As far as the piezoelectric actuator with in-plane motion is concerned, when a voltage is applied to one of the piezoelectric elements in the direction of polarization vector, the piezoelectric material produces actuation strain in directions 1 and 2, and thus the actuator contracts or expands correspondingly in the same directions (Fig. 1). The induced force due to coupling actuates the elastic structure and generates in-plane motions.

According to the principle of virtual work of a deformed piezoelectric medium, the weak formulation of the equilibrium equations can be given as follow:

$$\int_\Omega \varepsilon_{ij}(u)C_{ijkl}\varepsilon_{kl}(v)d\Omega + \int_\Omega \varepsilon_{ij}(v)e_{kij}(\nabla\phi)_k d\Omega = \int_\Omega p_i v_i d\Omega + \int_S t_i v_i dS, \tag{3}$$

$$\int_\Omega (\nabla\varphi)_k e_{kij}\varepsilon_{ij}(u)d\Omega - \int_\Omega (\nabla\varphi)_k \lambda_{ik}(\nabla\phi)_i d\Omega = \int_S \varphi_i q_i dS, \tag{4}$$

where p and t represent body force and mechanical traction, and q denotes the electric body charge. v and φ are virtual displacement and virtual electric change, respectively.

Using finite element formulation, the following equilibrium equations for the piezoelectric medium is in matrix form can be obtained as:

$$\begin{bmatrix} \mathbf{K}_{uu} & \mathbf{K}_{u\varphi} \\ \mathbf{K}_{u\varphi}^T & \mathbf{K}_{\varphi\varphi} \end{bmatrix} \begin{Bmatrix} \mathbf{U} \\ \mathbf{\Phi} \end{Bmatrix} = \begin{Bmatrix} \mathbf{F} \\ \mathbf{Q} \end{Bmatrix} \tag{5}$$

where $\mathbf{K}_{uu}$, $\mathbf{K}_{u\varphi}$ and $\mathbf{K}_{\varphi\varphi}$ are the stiffness, piezoelectric coupling and dielectric matrices, respectively, $\mathbf{U}$ and $\mathbf{\Phi}$ represent the vectors of nodal displacements and nodal electric potentials, and $\mathbf{F}$ and $\mathbf{Q}$ are the vectors of applied nodal forces and nodal electric charges. For smart piezoelectric plates used as actuators, it is usual to assume that the electric field is constant across the thickness and aligned normal to the mid-plane. In other words, the electric potential is assumed to be linearly polarized from the top electrode of the plate to its bottom electrode. As a result, $\mathbf{\Phi}$ becomes a known vector for the actuator design. It is also noted that $\mathbf{Q}$ contains only internal electric charges. Thus, the mechanical and electric problems are decoupled and only the first set of equation need to be solved numerically, because in this case the dielectric properties involved in the second set of equations can be ignored.

$$\mathbf{K}_{uu}\mathbf{U} + \mathbf{K}_{u\varphi}\mathbf{\Phi} = \mathbf{F}, \tag{6}$$

where the mechanical stiffness matrix and the piezoelectric coupling matrix can be written as

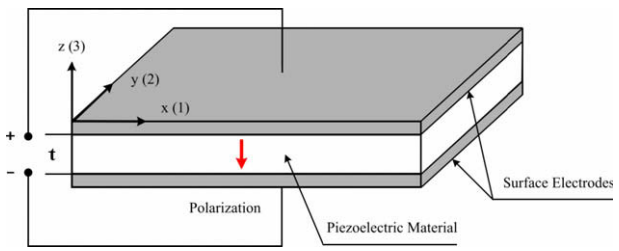

Fig. 1. Schematic diagram of a piezoelectric actuator.

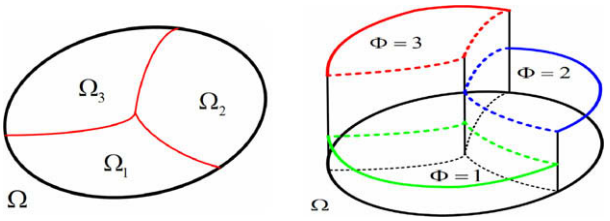

Fig. 2. Sub-domains and the piecewise constant functions.

$$(\mathbf{K}_{uu})^e = \int_\Omega \mathbf{B}_u^{\mathrm{T}} \mathbf{C} \mathbf{B}_u d\Omega = \sum_{e=1}^{N} \left[\int_{\Omega^e} (\mathbf{B}_u^{\mathrm{T}})^e \mathbf{C}^e (\mathbf{B}_u)^e d\Omega \right], \quad e = 1, 2, \ldots N \tag{7}$$

$$(\mathbf{K}_{u\varphi})^e = \int_\Omega \mathbf{B}_u^{\mathrm{T}} \mathbf{e}^{\mathrm{T}} \mathbf{B}_\varphi d\Omega = \sum_{e=1}^{N} \left[\int_{\Omega^e} (\mathbf{B}_u^{\mathrm{T}})^e (\mathbf{e}^{\mathrm{T}})^e (\mathbf{B}_\varphi)^e d\Omega \right], \quad e = 1, 2, \ldots N \tag{8}$$

In the design of piezoelectric actuators with in-plane motion, it is a common practice to calculate the actuation force as follows if the voltage is applied as the input to the piezoelectric material

$$\mathbf{F}_{pzt}^e = -\left[\int_{\Omega^e} (\mathbf{B}_u^{\mathrm{T}})^e (\mathbf{e}^{\mathrm{T}})^e (\mathbf{B}_\varphi)^e d\Omega \right] \mathbf{\Phi}^e = \left[\int_{\Omega^e} (\mathbf{B}_u^{\mathrm{T}})^e (\mathbf{e}^{\mathrm{T}})^e d\Omega \right] \mathbf{E}^e. \tag{9}$$

In this way, the global equilibrium equation is changed to the following form:

$$\mathbf{K}_{uu}\mathbf{U} = \mathbf{F} + \mathbf{F}_{pzt}^e, \tag{10}$$

where the electric field is related to the electric potential by

$$\mathbf{E}^e = -grad(\varphi) = -B_\Phi \hat{\varphi}. \tag{11}$$

Since the electric potential is supposed to distribute linearly along the thickness of the piezoelectric plate (Fig. 1), and the electric field vector for any element is given as

$$\mathbf{E}^e = [0 \ 0 \ v^e/t]^{\mathrm{T}}, \tag{12}$$

where v^e is the applied related voltage and t is the thickness of the piezoelectric plate. φ is the electric potential, $\hat{\varphi}$ is the vector of nodal potentials and B_Φ is the strain matrix.

3. Piecewise constant multiphase formulation

With standard level set methods [32,34], the multiphase interfaces will be implicitly tracked by representing them respectively as the zero level sets of some Lipschitz continuous functions of higher dimension [48]. However, in this study, the different phases are identified only using one indicator function including level sets of piecewise constants in the design domain [23,24,43,44].

It is assumed that Ω is completely divided into a set of sub-regions $\{\Omega_i\}_{i=1}^n$ (such as $i = 1,2,3$ in Fig. 2). To identify the different sub-domains involved in Ω, it needs to find an indicator function Φ which takes the following constant values such that:

$$\Phi(x) = i, \quad x \in \Omega_i \quad (i = 1, 2, \ldots, n). \tag{13}$$

A set of characteristic functions χ_i (Fig. 3) associated with Φ are then defined as follows for the sake of uniquely identifying the different sub-domains

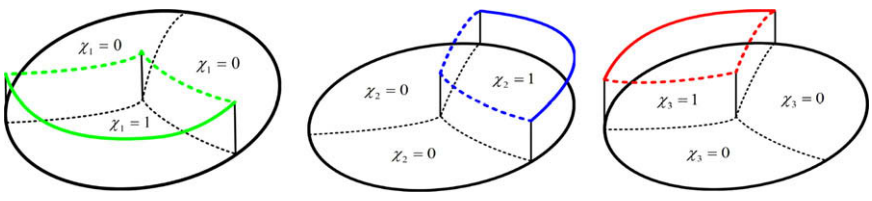

Fig. 3. Corresponding characteristic function for each sub-domain.

$$\chi_i(\Phi) = \frac{1}{\alpha_i}\prod_{j=1,j\neq i}^{n}(\Phi - j) \quad \text{and} \quad \alpha_i = \prod_{k=1,k\neq i}^{n}(i-k). \tag{14}$$

Thus, any of a piecewise constant function ψ is defined in terms of the characteristic functions

$$\psi(\Phi) = \sum_{i=1}^{n} c_i\chi_i(\Phi). \tag{15}$$

The curves separating the regions can then be described via the discontinuities of Φ taking a set of constant values. For instance, the function for a three phase's problem with two different solid materials can be defined by

$$\psi(\Phi) = \sum_{i=1}^{3} c_i\chi_i(\Phi) = (c_1\chi_1(\Phi) + c_2\chi_2(\Phi) + c_3\chi_3(\Phi)), \tag{16}$$

where

$$\chi_1(\Phi) = (\Phi-2)(\Phi-3)/\alpha_1 \quad \text{and} \quad \alpha_1 = (1-2)(1-3) = 2, \tag{17}$$

$$\chi_2(\Phi) = (\Phi-1)(\Phi-3)/\alpha_2 \quad \text{and} \quad \alpha_2 = (2-1)(2-3) = -1, \tag{18}$$

$$\chi_3(\Phi) = (\Phi-1)(\Phi-2)/\alpha_3 \quad \text{and} \quad \alpha_3 = (3-1)(3-2) = 2, \tag{19}$$

where c_i ($i = 1,2,\ldots,n$) are the pre-defined coefficients no need to be updated together with the design variables [24]. In this work, the values of c_i for three different phases are defined as $c_1 = 0.001$, $c_2 = 0.5$ and $c_3 = 1$ [51]. It is noted that the length of curves surrounding each sub-domain Ω_i and the area of each sub-domain Ω_i can be expressed, respectively, as follows:

$$|\partial\Omega_i| = \int_\Omega |\nabla\chi_i(\Phi)|dx \quad \text{and} \quad |\Omega_i| = \int_\Omega \chi_i(\Phi)dx \tag{20}$$

4. Topology optimization of multi-material actuators

In this work, the PCLSM based topology optimization method is used to seek the optimum distribution of a given portion of materials by simultaneously determining the distributions of the elastic, piezoelectric and void phases under specified supports and applied loads.

The design domain of multi-material piezoelectric actuators is illustrated in Fig. 4, where an artificial spring model [38] consisting of a spring with a given stiffness is mounted at the output port position to simulate the reaction force from a workpiece.

4.1. Optimization formulation of multi-material actuators

To ensure that Eq. (14) is a unique representation of ψ and also to ensure the indicator function Φ converges to piecewise constant values at convergence, the function Φ is required to satisfy the following constraint at every point $x \in \Omega$

$$K(\Phi) = 0, \tag{21}$$

where

$$K(\Phi) = (\Phi-1)(\Phi-2)\ldots(\Phi-n) = \prod_{i=1}^{n}(\Phi-i). \tag{22}$$

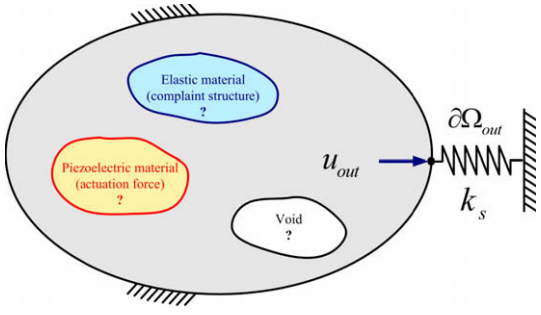

Fig. 4. Design domain of multi-material smart actuators.

In this way, the constraint in Eq. (21) can be used to guarantee there is no vacuum and overlap between different material phases [23,24], compared with the conventional level set methods using other schemes to avoid vacuum and overlap [54,46,48]. The design of multi-material piezoelectric actuators is formulated as a constrained minimization problem with respect to the design variable Φ as follows:

$$\begin{cases} \underset{(\Phi)}{\text{Minimize}}: & J(u,\Phi)=\int_\Omega \psi(\Phi) f(u,v)d\Omega+\beta\int_\Omega|\nabla\Phi|d\Omega \\ \text{Subject to}: & \begin{cases} G_0(\Phi)=K(\Phi)=0, \\ G_1(\Phi)=\int_\Omega\psi(\Phi)d\Omega-V_1^*\leqslant 0, \\ G_2(\Phi)=\int_\Omega\psi(\Phi)d\Omega-V_2^*\leqslant 0, \\ \text{Equilibrium equation}. \end{cases} \end{cases} \tag{23}$$

In this work, only Φ is regarded as the design variable to be updated and c is a pre-determined value [50,51]. V_1^* and V_2^* are the volume constraints related to elastic and piezoelectric materials, respectively. It is noted that the second term on the right-hand side of the objective formulation, the sum of the perimeters of the sub-domain boundaries, is used as a penalization to regularize the solution space because of the ill-posedness of the original problem [24]. It is necessary to use the penalization parameter $\beta > 0$ to control the influence of the regularization term, and thus to control the jumps and the length of the sub-domain boundaries. The equilibrium equation is defined in terms of Eq. (10) as

$$\bar{a}(u,v,\Phi)=\bar{l}(v,\phi,\Phi), \tag{24}$$

where

$$\bar{a}(u,v,\Phi)=\int_\Omega \psi(\Phi)\varepsilon_{ij}(u)^{\mathrm{T}}C_{ijkl}\varepsilon_{kl}(v)d\Omega \tag{25}$$

$$\bar{l}(v,\phi,\Phi)=\int_\Omega \psi'(\Phi)|\nabla\Phi|\tau v d\Omega+\int_\Omega \psi(\Phi)(\nabla\phi_k)^{\mathrm{T}}e_{kij}^{\mathrm{T}}\varepsilon_{ij}(v)d\Omega, \tag{26}$$

where ∇ is the gradient operator, and v is the virtual displacement field. u and ϕ are the displacement field and electric potential vector, respectively. Φ is the indicator function including piecewise constants, and ψ represents any piecewise constant in Eq. (15).

4.2. Design sensitivity analysis

Using the augmented Lagrangian function method [31], the constrained minimization problem is converted to the following unconstrained minimization problem

$$\begin{aligned} L(\Phi,\lambda_0,\mu_0,\lambda_1,\mu_1,\lambda_2,\mu_2)=J(u,\Phi)+\bar{a}(u,v,\Phi)-\bar{l}(v,\phi,\Phi)+\lambda_0\int_\Omega G_0(\Phi)d\Omega+\frac{1}{2\mu_0}\int_\Omega G_0(\Phi)^2d\Omega+\lambda_1G_1(\Phi)+\frac{1}{2\mu_1} \\ \times[G_1(\Phi)]^2+\lambda_2G_2(\Phi)+\frac{1}{2\mu_2}[G_2(\Phi)]^2, \end{aligned} \tag{27}$$

where Ω denotes a smooth bounded open set. λ_0, λ_1 and λ_2 are the Lagrangian multipliers, and μ_0, μ_1 and μ_2 are the penalization parameters, respectively. Then, the minimization of L can be obtained by finding a saddle-point of the augmented Lagrangian functional, which means to find the stationary point of the Lagrangian by letting $\delta L = 0$ with respect to the design variable Φ, the Lagrangian multipliers and the penalization parameters, respectively

(1) The state equation can be found by satisfying $\partial L/\partial v = 0$

$$\bar{a}(u,v',\Phi)=\bar{l}(v',\phi,\Phi). \tag{28}$$

(2) The adjoint equation can be obtained by applying $\partial L/\partial u = 0$

$$J(u',\Phi)=\bar{a}(u',v,\Phi). \tag{29}$$

(3) By applying $\partial L/\partial(\lambda_0,\lambda_1,\lambda_2) = 0$, the equations of the inequality conditions are given as

$$\begin{aligned} &\lambda_0\int_\Omega K(\Phi)d\Omega=0, \quad \lambda_0\geqslant 0 \\ &\lambda_1\left(\int_\Omega\psi(\Phi)d\Omega-V_1^*\right)=0, \quad \lambda_1\geqslant 0 \\ &\lambda_2\left(\int_\Omega\psi(\Phi)d\Omega-V_2^*\right)=0, \quad \lambda_2\geqslant 0 \end{aligned} \tag{30}$$

(4) To find the optimality criteria via updating the piecewise constant level set function, the strong formulation of the optimality criteria can be found by letting

$$\frac{\partial L}{\partial \Phi} = J(u,\Phi') + \bar{a}(u,v,\Phi') - \bar{l}(v,\phi,\Phi') + \lambda_0 \int_\Omega G_0' d\Omega + \lambda_1 G_1' + \lambda_2 G_2' = 0. \tag{31}$$

According to Eqs. (23) and (31) can further be rewritten as

$$\frac{\partial L}{\partial \Phi} = \int_D \vartheta(\Phi,\lambda_0,\mu_0,\lambda_1,\mu_1,\lambda_2,\mu_2)\cdot\Phi' d\Omega = 0, \tag{32}$$

where ϑ can be found by deriving the related equations in Eq. (23), respectively, as

$$\vartheta = \psi'(\Phi)f(u,v) + \beta\left(\nabla\cdot\frac{\nabla\Phi}{|\nabla\Phi|}\right) - \nabla(\tau v)\cdot\frac{\nabla\Phi}{|\nabla\Phi|} - \left(\nabla\cdot\frac{\nabla\Phi}{|\nabla\Phi|}\right)\tau v + \psi'(\Phi)(\nabla\phi_k)^{\mathrm{T}} e_{kij}^{\mathrm{T}}\varepsilon_{ij}(v) + \psi'(\Phi)\varepsilon_{ij}^{\mathrm{T}}(u)C_{ijkl}\varepsilon_{kl}(v) + \lambda_0 K'(\Phi) + \lambda_1\psi'(\Phi) + \lambda_2\psi'(\Phi). \tag{33}$$

The state and adjoint equations in (28) and (29) need to be solved using the finite element method in order to obtain the unknown displacement vectors u and v, respectively, in Eq. (33). For a three-phase piezoelectric actuator in this work, we have

$$\psi'(\Phi) = (c_1 - 2c_2 + c_3)\Phi + 0.5(-5c_1 + 8c_2 - 3c_3), \tag{34}$$

$$K'(\Phi) = (3\Phi^2 - 12\Phi + 11) \tag{35}$$

An *ad hoc* scheme for updating the Lagrangian multipliers and the penalty parameters are, respectively, given as follows [44,50,27]:

$$\lambda_0^{k+1} = \lambda_0^k + \frac{1}{\mu_0^k}[K(\Phi)] \tag{36}$$

$$\lambda_1^{k+1} = \lambda_1^k + \frac{1}{\mu_1^k}\left[\int_\Omega \psi(\Phi)d\Omega - V_1^*\right], \tag{37}$$

$$\lambda_2^{k+1} = \lambda_2^k + \frac{1}{\mu_2^k}\left[\int_\Omega \psi(\Phi)d\Omega - V_2^*\right], \tag{38}$$

$$\mu_i^{k+1} \in (0,\mu_i^k), \quad i = 1,2,3. \tag{39}$$

It is noted that the derivative of the augmented Lagrangian function agrees with that of the objective function if all the constraints are satisfied. To ensure the decent of the objective function, a proper velocity field $d\Phi/dt = v$ should be selected for the piecewise constant level set function. As indicated in the literature [47,2], the simplest way is to directly determine a steepest descent direction by letting

$$v = \Phi' = -\vartheta(\Phi,\lambda_0,\mu_0,\lambda_1,\mu_1,\lambda_2,\mu_2) \tag{40}$$

so as to guarantee a descent direction of the augmented Lagrangian function (objective), because

$$\frac{\partial L}{\partial \Phi} = -\int_\Omega [\vartheta(\Phi,\lambda_0,\mu_0,\lambda_1,\mu_1,\lambda_2,\mu_2)]^2 d\Omega \leqslant 0. \tag{41}$$

Therefore, the minimization problem can be solved by using the following (or equivalent) scheme to update the level set function Φ [24]:

$$\frac{\partial\Phi(x,t)}{\partial t} + v(x) = 0 \Longleftrightarrow \frac{\Phi^{n+1} - \Phi^n}{\Delta t} + v(x) = 0, \quad \Phi(x,0) = \Phi_0(x), \tag{42}$$

where Δt represents a small positive number which can be determined by using trial and error [24,44]. It can be seen that the differential equation in (42) is a type of partial differential equations (PDE) similar to that in the conventional level set methods [36].

5. A semi-implicit additive operator splitting scheme

Amongst many methods for solving Eq. (42), it is well known that the conventional explicit scheme has a strict limitation on time-marching step size and it is only numerically stable for very small time steps satisfying the CFL condition [25,36], which will lead to poor computational efficiency and limits its practical applications. This section employs a

semi-implicit scheme to enable the discrete level set processing so as to update the level sets of piecewise constant types in the indicator function Φ. The semi-implicit scheme was originally presented in image processing technologies and computer version by Lu et al. [25], and later independently developed in a different context of image processing [52]. The basic idea behind the AOS scheme is to split the m-dimensional spatial operator into a set of *one*-dimensional space discretizations that can be efficiently solved with a well-founded Gaussian elimination algorithm named *Thomas Algorithm* [52]. The AOS scheme inherits several favorable features from their original image diffusion process [25], which treats all coordinate axes equally and can be easily implemented in arbitrary dimensions. A similar semi-implicit scheme has been applied to shape and topology optimization of compliance designs of single material structures [27]. This study applies the AOS scheme to more general shape and topology optimization problems of multiphysics and multi-material.

Considering Eqs. (40) and (42), the semi-implicit AOS scheme for updating the function Φ is given as [52,27]

$$\Phi^{k+1} = \frac{1}{m}\sum_{l=1}^{m}[I - m\Delta t\xi A_l(\Phi^k)]^{-1}[\Phi^k + \Delta t\, v(x)], \tag{43}$$

where ξ is the weighting factor for the diffusion term, and m represents the number of dimensions. A_l is introduced as the matrix to measure the derivatives along the lth coordinate axis. All these operators are composed of a strictly diagonally dominant tridiagonal linear system. With the definition of $A_l(\Phi^k) = a_{ij}(\Phi^k)$, $a_{ij}(\Phi^k)$ can be expressed as follows:

$$a_{ij} = \begin{cases} \frac{1}{h_l^2}\frac{2}{(|\nabla\Phi|_i^k + |\nabla\Phi|_j^k)}, & j \in N_l(i) \\ 0, & \text{else} \\ -\frac{1}{h_l^2}\sum\limits_{n\in N_l(i)}\frac{2}{(|\nabla\Phi|_i^k + |\nabla\Phi|_n^k)}, & i = j. \end{cases} \tag{44}$$

The operator A can be spilt into two components in x and y directions, respectively, as

$$A_1 = \frac{\partial}{\partial x}\left(\frac{1}{|\nabla\Phi|^k}\frac{\partial}{\partial x}\right), \quad A_2 = \frac{\partial}{\partial y}\left(\frac{1}{|\nabla\Phi|^k}\frac{\partial}{\partial y}\right). \tag{45}$$

In numerical implementation, the level set function Φ can be updated as

$$\Phi^{k+1} = \frac{1}{2}[\varphi_1(\Phi^{k+1}) + \varphi_2(\Phi^{k+1})]. \tag{46}$$

To simplify the above equation, let

$$\varphi_1(\Phi^{k+1}) = (I - 2\Delta t\xi A_1(\Phi^k))^{-1}[\Phi^k + \Delta t\, v(x)], \tag{47}$$

$$\varphi_2(\Phi^{k+1}) = (I - 2\Delta t\xi A_2(\Phi^k))^{-1}[\Phi^k + \Delta t\, v(x)]. \tag{48}$$

Then, $\varphi_1(\Phi)$ and $\varphi_2(\Phi)$ can be easily solved with the following equations using the *Thomas method* as a Gaussian elimination algorithm for tridiagonal systems [52].

$$[I - 2\Delta t\xi A_1(\Phi^k)]\varphi_1(\Phi) = \Phi^k + \Delta t\, v(x), \tag{49}$$

$$[I - 2\Delta t\xi A_2(\Phi^k)]\varphi_2(\Phi) = \Phi^k + \Delta t\, v(x) \tag{50}$$

As described above, the AOS scheme is time stable by satisfying all practical discrete scale-space for arbitrary time step sizes in solving Eq. (42), and it can enable a much large time step size due to the total relaxation of the CFL condition. Weickert et al. [52] have proved that under typical accuracy requirements AOS schemes are at least several times as efficient as the conventional explicit schemes. Although the AOS scheme does not suffer from any time step size restriction because of the total relaxation of the CFL condition, in practice it is undesirable to use too large time steps due to the linearization of the scheme, as it will lead to poor rotation invariance in non-linear diffusion problems [52].

It is well known that the conventional discrete level set methods have a tendency to lose the shape of the level set surface and as a result lead to too flat and (or) too steep gradients [45], due to unwanted numerical diffusion caused by the local approximation scheme (e.g. up-wind schemes). In general, it needs to regularize the original surface using a time-consuming re-initialization scheme [32,34] to ensure a good approximation of the curvature of the free front, so as to resurrect the behavior of the level set surface in the neighbor of the front while keeping the zero level set unchanged. The error accumulated from periodic re-initialization may appreciably move the front if the common iterative procedure is used to retain a signed distance function. Furthermore, the re-initialization algorithm will forbid the nucleation of new holes inside the material domain [9,30]. But the present AOS scheme is capable of ensuring a globally smooth level set surface, as the underlying problem is evaluated over the entire level set function and the steep gradients is obtained on the fixed extended design domain. Hence, it is unlikely to lose the surface without applying the re-initialization procedures, which is conventionally caused by local numerical approximation methods when explicit time-marching schemes like the up-wind method are employed [47,2].

6. Numerical implementation

6.1. Numerical procedure

The major steps for the present level set method can be outlined as follows:
For $k = 0, 1, 2 \ldots$

(1) Solve the state and adjoint equations using the finite element method to get the displacement vectors u and v in Eq. (33), respectively;
(2) Perform design sensitivity analysis to obtain the derivatives $H'(\Phi)$ and $K'(\Phi)$ in Eqs. (34) and (35), and then to determine the solution of ϑ in Eq. (40);
(3) Use the AOS scheme to update the level set function Φ starting from Φ^k in Eq. (40), so as to minimize the objective function in Eq. (23);
(4) Renew the Lagrange multipliers λ_0, λ_1 and λ_2 and the related penalty parameters μ_0, μ_1 and μ_2 in Eqs. (36)–(39);
(5) Check convergence, if satisfied, stop, else, go to step (1).

6.2. The piecewise constant constraint

As aforementioned, the piecewise constant constraint $K(\Phi) = 0$ plays an important role in the optimization problem because it actually serves as a penalization to ensure that each point $x \in \Omega$ can converge to one and only one phase, so as to ensure that there is no vacuum and overlap between different material phases [24,43,50,51]. If $K(\Phi) = 0$ is satisfied, Eq. (15) will lead to a unique representation of the piecewise constant function $H(\Phi)$ at convergence and different values of Φ correspond to different function values $H(\Phi)$. It can be easily understood that the original constraint $K(\Phi) = 0$ in Eq. (23) can be replaced by $K^n(\Phi) = 0$ (n is an integer larger than 1). Fig. 5 shows the shapes of $K^n(\Phi)$ when n has different values such as 2, 4 and 6. For all these cases, it can be seen that the constant values of function Φ can converge to 1, 2 and 3 when the value of $K^n(\Phi)$ approaches to 0. However, the figure shows that if n has a larger value (i.e. $n = 6$) the penalization effect of the piecewise constant constraint will degenerate when Φ deviates from the piecewise constant values such as 1, 2 and 3. The numerical process indicates that for a larger n the stability of the convergence is slightly improved, but more iteration is required for the level set value on each point to converge to the corresponding phase exactly. The possible reason for this is that the gradient of $K^n(\Phi)$ decreases as the value of n is increased. Thus, $n = 2$ is used here to achieve a faster convergence speed, to strengthen the penalization effect and to guarantee a moderate stability.

6.3. Numerical examples

Two widely studied examples are used to illustrate the application of the present method to shape and topology optimization of piezoelectric actuators. The objective is to simultaneously distribute non-piezoelectric, piezoelectric and void materials without pre-defined shapes and topologies in the design domain. In each of the examples, we adopt the same material model only for the sake of simplicity. However, it is straightforward to apply the present level set method to shape and topology optimization problems including any kinds of engineering materials. It should be pointed out that the units of all the parameters can be defined flexibly, but they should remain unchanged and uniformly during all stages such as formulation modeling, finite element analysis and optimization procedure. In this research, the standard PZT-5A model is used

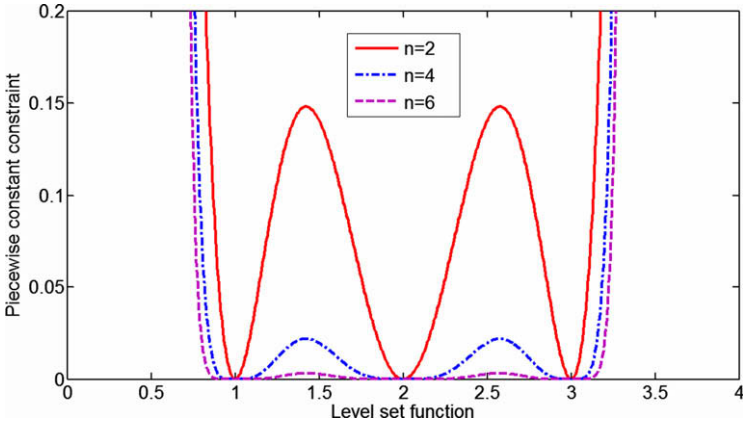

Fig. 5. Piecewise constant constraint with different n values.

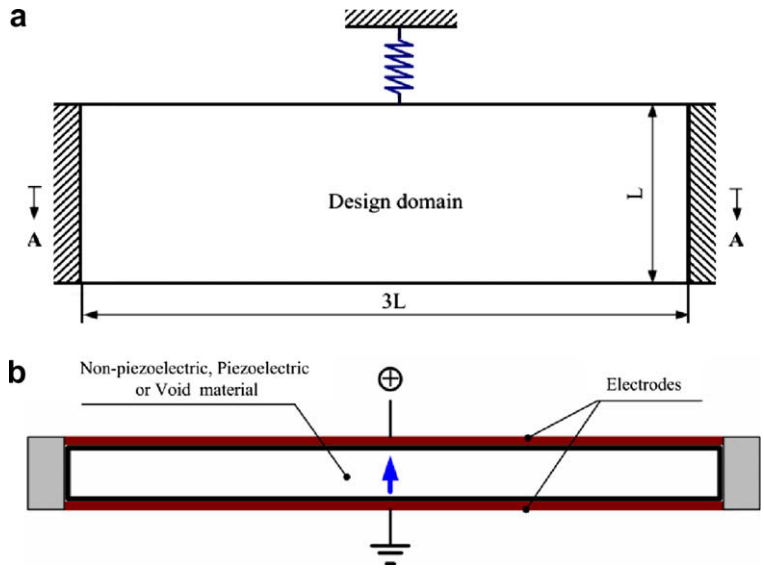

Fig. 6. (a) Design domain of the multi-material smart actuator. (b) "A-A" section of the multi-material design domain.

for the piezoelectric material and Aluminum is used for the elastic material. The voltage is applied to generate the piezoelectric actuation via the electrodes attached to the entire upper and lower surfaces of the design domain, because the piezoelectric electrodes are not known in advance. The termination criterion of iteration is the relative difference of the objective function values between two successive iterations is less than 0.001.

6.3.1. Example 1

The design domain is shown as Fig. 6(a) with fixed mechanical boundary conditions at left and right sides, and it is discretized with 150 × 50 isotropic plate finite elements with a uniform thickness 10 μm. The piezoelectric field is displayed in Fig. 6(b) with an applied voltage 500 V. It should be pointed out that the actual boundary lengths are 600 × 200 μm, but we have scaled the sizes in Fig. 7 only for the sake of displaying the level set surface more clearly by fully taking advantage of the Matlab function. The volume constraints for elastic and piezoelectric material are specified as 15% and 10%, respectively. The constant values 1, 2 and 3 are used as different piecewise functions to represent the void, elastic and piezoelectric material,

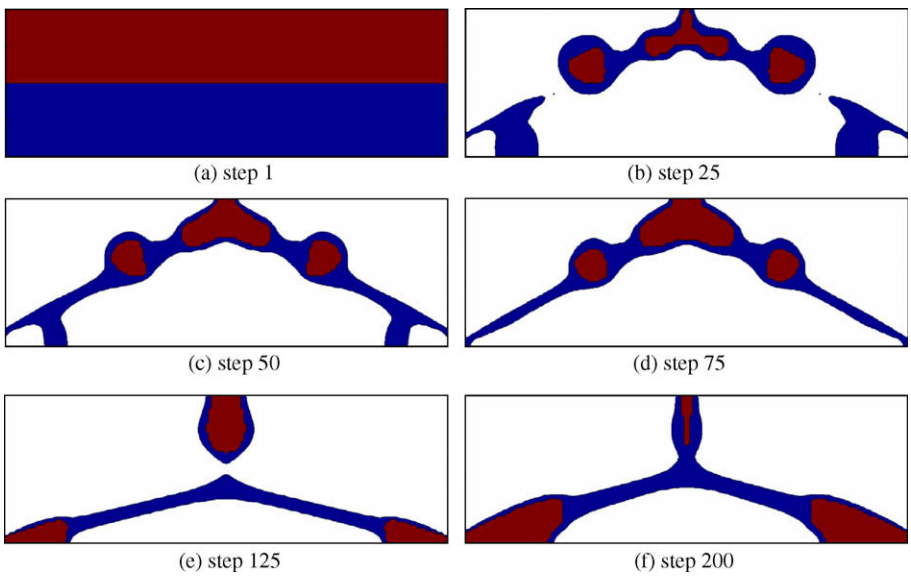

Fig. 7. Topologies of the multi-material smart actuator.

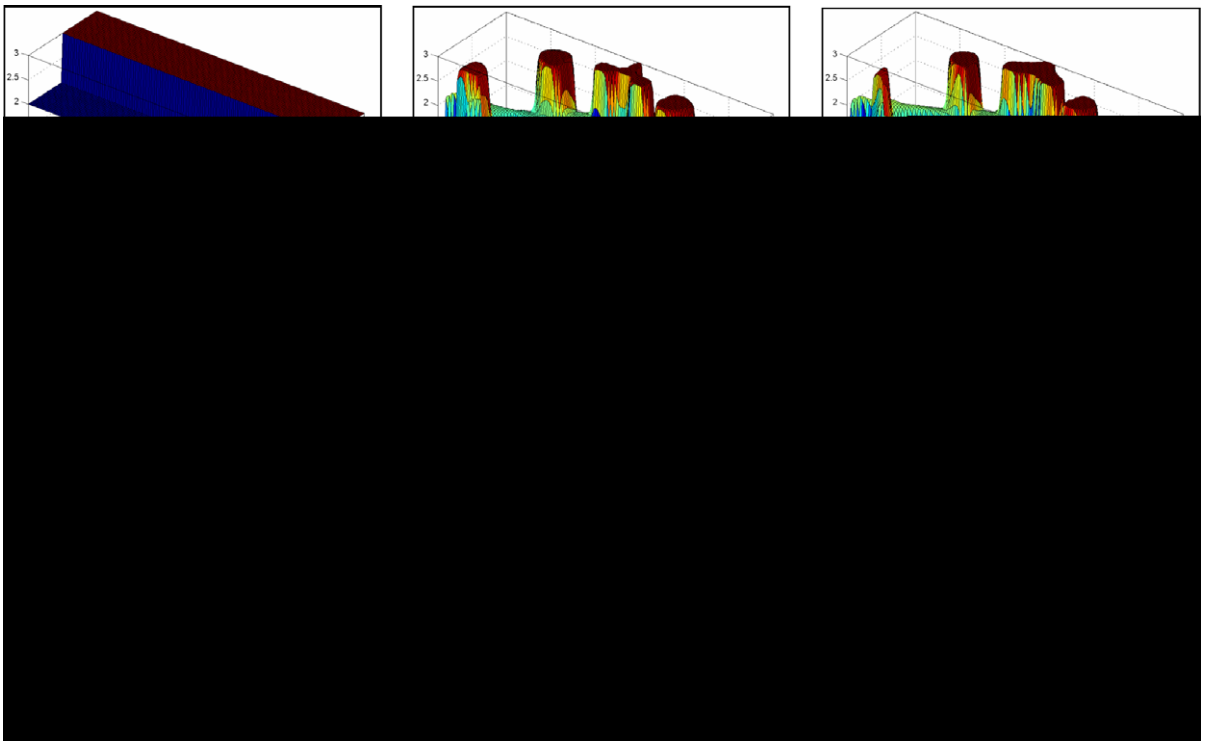

Fig. 8. Level set surfaces of the multi-material smart actuator.

respectively. In the AOS scheme, the parameter $\beta = 0.005$ is applied to control the influence of the regularization term, and the time step size is selected as $\Delta t = 5$ to enable the advancement of the piecewise constant level set function Φ.

The evolvement process of the topologies and the corresponding level set surfaces are shown in Figs. 7 and 8, respectively. The constant value function "1" represents the level set of the void region, "2" denotes the level set of the passive elastic material and "3" is the level set of the piezoelectric material. It can be seen that the proposed piecewise level set method is able to distribute the non-piezoelectric material and the piezoelectric material in the fixed extended design domain at the same time. As a result, the shape and topology of passive host compliant structure and placements, shapes and topologies of the PZT actuators can be optimized simultaneously. The passive structure can be regarded as a compliant mechanical multiplier to enlarge the small output stroke produced by the PZT material. Furthermore, we can find that the present piecewise constant level set method still retains the favorable characteristics of the implicit free boundary representation scheme [32,36]. For instance, the shape and topology optimization can be processed at the same time via a smooth advancement of the explicit boundaries. Fig. 9(a) displays the convergent history of the design objective to have been maximized at the specified output position, in which the optimal value 9.87 μm is obtained after 200 iterations. The volume ratios in relation to the elastic and piezoelectric material in Fig. 9(b) show that the both constraints are conservative, where the upper curve for the elastic material converges from 0.5 to 0.15 and the lower is from 0.5 to 0.1.

Compared to the conventional level set method [32,36,34], the proposed level set method is free from the limitation of the CFL condition so that a large time step size is applied to speed up the convergence process. If the same problem is solved using the conventional level set method with explicit up-wind scheme [48], it needs at least 2000 iterations to achieve the optimal design under the same convergence condition. In addition, it is unnecessary to apply the re-initialization procedures [36] periodically to retain the regularization of the level set surface, and the velocity extension scheme is also avoided. In particular, the present method is able to generate new holes inside the design domain. This is in contrast to the conventional level set method that is unable to create new holes inside the material domain because no mechanism was included for nucleation purpose [48,2,26], and some additional variation schemes, such as the bubble method [13] or the topological derivative [41], need to be incorporated to add new holes.

6.3.2. Example 2

The design domain of the multi-material actuator is defined in Fig. 10(a) with a square of 600 μm × 600 μm and discretized with 100 × 100 quadrilateral plate elements in order to display the entire mechanism. The design domain is given a uniform thickness 10 μm. The left, top and bottom sides are fixed as the Dirichlet boundaries, and the right side is a non-homogenous Neumann boundary. The piezoelectric field is described in Fig. 10(b) with a uniformly applied voltage 500 V on the upper surface of the PZT plate. The volume constraints for the elastic material and the piezoelectric material are de-

Fig. 9. (a) Iteration curve of the design objective function. (b) Iteration curve of the different volume ratios.

Fig. 10. (a) Design domain of the multi-material smart actuator.(b) Design domain of the multi-material smart actuator.

fined as 17.5% and 10%, respectively. The void, elastic and piezoelectric phases are represented using different piecewise constant values 1, 2 and 3, respectively. $\beta = 0.005$ is used to weight the regularization term, and $\Delta t = 5$ is used as the time step size to enable the evolvement of the piecewise constant level set function Φ.

The topologies and the related level set surfaces are displayed in Figs. 11 and 12, respectively. We can find that all the designs are characterized with a smooth boundary, and the shape and topology optimization can be performed at the same time to get an optimized structure with multi-material distribution, which are the two main merits of the level set-based implicit representation [48]. Fig. 12 indicates that the piecewise constant type function Φ can approach the constant values 1, 2 and 3 on convergence, respectively. In such a way, the optimization can be regarded as a numerical process of distributing the elastic and piezoelectric materials flexibly in the fixed extended domain until the passive coupling structure and the PZT actuators are optimized simultaneously. Furthermore, a relatively large time step size can be applied to speed up the optimization process, because the semi-implicit scheme rather than the explicit scheme is used to solve the initial value problem with a total

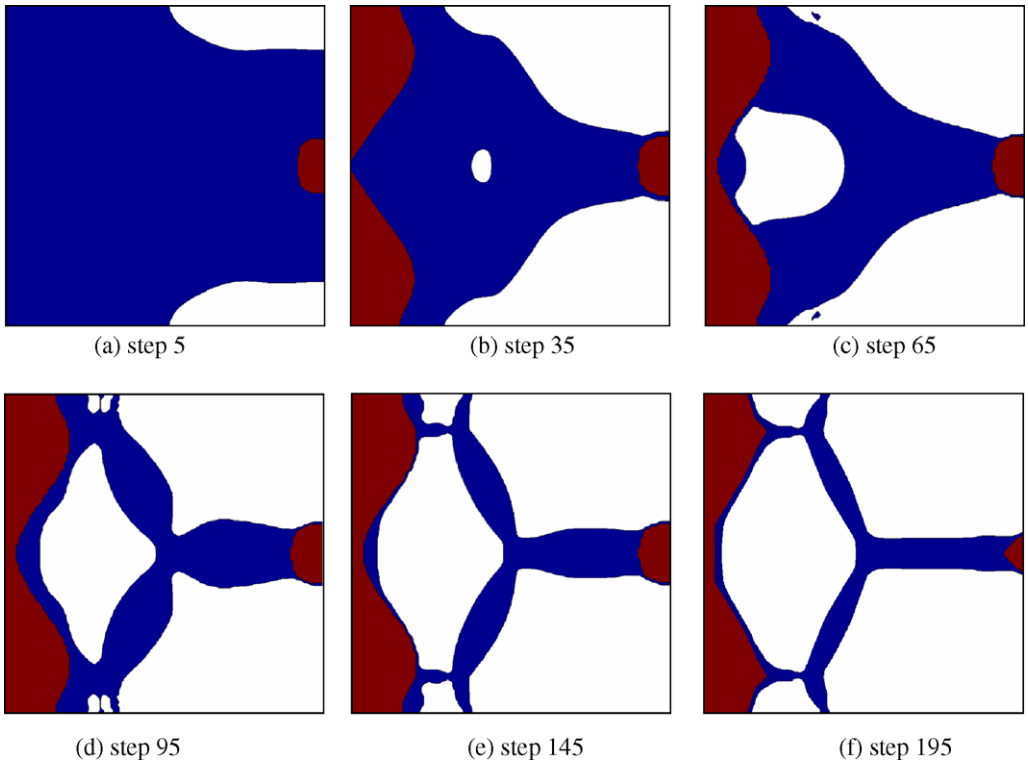

Fig. 11. Topologies of the multi-material smart actuator.

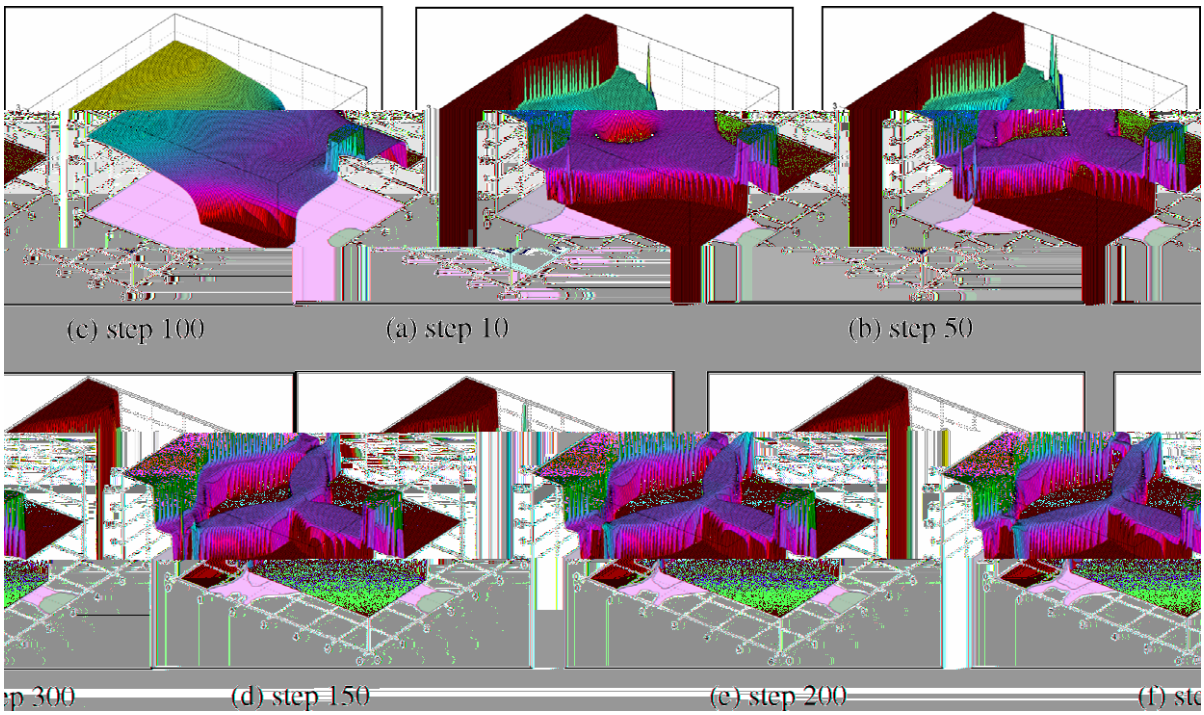

Fig. 12. Level set surfaces of the multi-material smart actuator.

relaxation of the CFL condition [24,44]. It can be seen from Fig. 11 that new holes can be created inside the design domain which prevents the design from some local minima. In addition, the re-initialization procedures and the velocity extension scheme are also eliminated from the present level set method. The final design (Fig. 13(a)) is obtained after 309 iterations with a displacement output 35.14 μm at the specified direction, and the volume constraints are conservative (Fig. 13(b)).

To further demonstrate the influence of the parameter β on the optimal design, we set the parameter to be 0.01, 0.001, and 0.0001 to study the regularization effect, respectively, and the results are shown in Fig. 14. The corresponding iteration numbers are 256, 332 and 378, respectively, and the objective values are 34.51, 35.05 and 35.89. The numerical results demonstrate that a larger value can suppress the iteration oscillation and has a tendency of leading to a simpler topology with relatively less iteration, while a smaller value will indicate a less smooth design process and a final design with thin-bar like structural members and more iteration. Hence, β is mainly used to control the boundary smoothness as well as the complex of the final topology via the regularization term, which adjusts the boundary smoothness by "relaxing" the piecewise constant constraint so as to control the jumps between the transitions of the different constant function surfaces. In practical applications, more or less, the selection of β is a case of numerical experience. It should be noted that several factors may influence the boundary smoothness besides the parameter β such as Δt and μ_i [24,27].

In conventional level set methods, explicit schemes are usually applied to solve the Hamilton–Jacobi PDE to enable the discrete level set processing. One of the most important considerations is the time step size Δt that must be sufficiently small to satisfy the CFL condition. Spatially, the marching distance each time is no more than the smallest grid size. However, the present method driven by the semi-implicit AOS algorithm is able to totally relax the CFL condition. As a result, the semi-implicit AOS scheme is stable with any practically meaningful time steps. Three numerical cases (Fig. 15) are further used to study the influence of the time step on optimal design with a quadrilateral mesh of 100×100, where the parameter $\beta = 0.001$, the volume ratios for elastic and piezoelectric material are now defined as 0.1 and 0.2, respectively. It can be seen that the time step size involving in the present level set method also has an influence on the final design. Fig. 15(a) denotes the optimal design having a more complex topology which is obtained after 540 iterations using the smallest step size $\Delta t = 1$, Fig. 15(b) shows the design obtained after 270 iterations using the modest step size $\Delta t = 5$ which is characterized with a relatively simple topology, and Fig. 15(c) is the design related to the largest step size $\Delta t = 10$ which is obtained after 187 iterations with the simplest topology. Although the present method is in theory free from any time step restriction on solving the initial value problem, numerical experience in general should be included to determine a practical time step size,

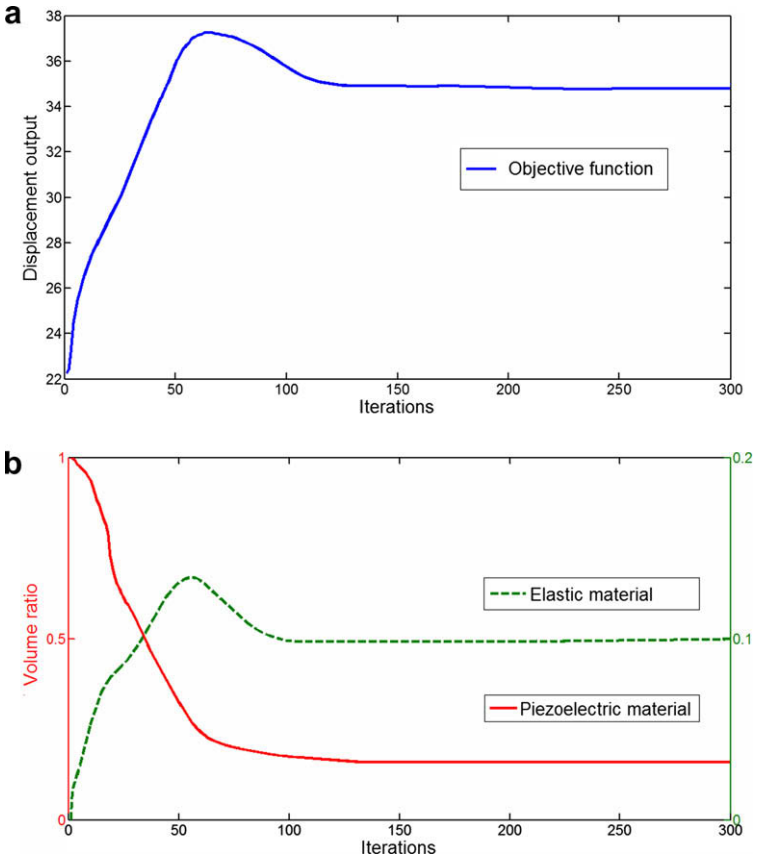

Fig. 13. (a) Iteration curve of the design objective function. (b) Iteration curve of the different volume ratios.

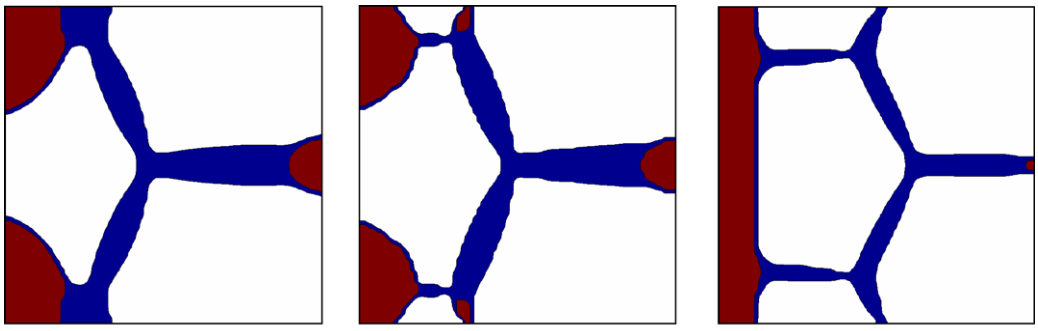

(a) β =0.01 (b) β =0.001 (c) β =0.0001

Fig. 14. Results with different parameter β.

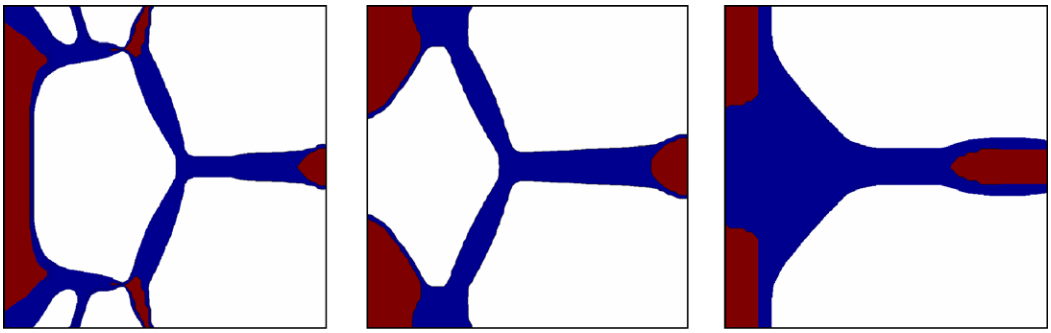

(a) Δt =1 (b) Δt =5 (c) Δt =10

Fig. 15. Designs with different step sizes.

because a too large step size may weaken the capability of the optimization method in describing topologies of sub-structures in optimization process [26]. In particular, it may delete some basic structure to have included the optimal topology configuration within the initial iterations. A too small step size will unnecessarily increase the computational cost, and the final design may involve a locally complex topology. As a matter of fact, the time step in the present piecewise constant level set method is somewhat similar to the *move limit* in the ad hoc updating scheme of optimality criteria methods [5], and it is easy to understand that the *move limit* has nothing to be with the CFL condition.

7. Conclusions

This paper proposes a level set-based multiphase method for shape and topology optimization of compliant piezoelectric actuators. An indicator function taking level sets of piecewise constant values is used to implicitly represent and identify the different design boundaries related to the multiple material regions in the design domain. Only one indicator function rather than several level set scalar functions is applied to identify all the boundaries between different phases via its discontinuities. The multi-material optimization problem is mathematically described as the minimization of a smooth energy functional under some specified constraints, to which the semi-implicit AOS scheme is applied. As a result, the design of the smart actuator is transferred to a numerical process of renewing the piecewise constant values until the piezoelectric actuators and the compliant amplifying structure are optimized. The numerical results show that the proposed level set method can remove several numerical difficulties associating with the solution of the Hamilton–Jacobi PDE in most conventional level set methods. The AOS scheme is stable for any practical time steps because the relaxation of the CFL condition in solving partial differential equations. The method in this study can also eliminate the time-consuming re-initializations in the conventional level set methods, and can create new holes inside the material domain. This method can be straightforwardly applied to optimization problems including more material phases.

Acknowledgments

This research was sponsored in part by the Australian Research Council (Grant No: DP0666683), the National Science Foundation of China (Grant No: 10728205), and the Research Grants Council of Hong Kong (CUHK416507).

References

[1] G.K. Ananthasuresh, L.L. Howell, Mechanical design of compliant microsystems – a perspective and prospects, Journal of Mechanical Design 127 (2005) 736–738.
[2] G. Allaire, F. Jouve, A.M. Toader, Structural optimization using sensitivity analysis and a level-set method, Journal of Computational Physics 194 (2004) 363–393.
[3] T. Belytschko, S.P. Xiao, C. Parimi, Topology optimization with implicitly function and regularization, International Journal for Numerical Methods in Engineering 57 (2003) 1177–1196.
[4] M.P. Bendsøe, N. Kikuchi, Generating optimal topology in structural design using a homogenization method, Computer Methods in Applied Mechanics and Engineering 71 (1988) 197–224.
[5] M.P. Bendsøe, O. Sigmund, Topology Optimization: Theory, Methods, and Applications, Springer, Berlin, Heidelberg, 2003.
[6] M.P. Bendsøe, O. Sigmund, Material interpolation schemes in topology optimization, Archive of Applied Mechanics 69 (1999) 635–654.
[7] A. Benjeddou, Advances in piezoelectric finite element modeling of adaptive structural elements: a survey, Computers & Structures 76 (2000) 347–363.
[8] M.J. Buehler, B. Bettig, G. Parker, Topology optimization of smart structures using a homogenization approach, Journal of Intelligent Material Systems and Structures 15 (2004) 655–667.
[9] M. Burger, B. Hacker, W. Ring, Incorporating topological derivatives into level set methods, Journal of Computational Physics 194 (2004) 344–362.
[10] R.C. Carbonari, E.C.N. Silva, S. Nishiwaki, Optimum placement of piezoelectric material in piezoactuator design, Smart Materials and Structures 16 (2007) 207–220.
[11] S. Canfield, M. Frecker, Topology optimization of compliant mechanical amplifiers for piezoelectric actuators, Structural and Multidisciplinary Optimization 20 (2000) 269–279.
[12] T.F. Chan, L.A. Vese, Active contours without edges, IEEE Transactions on Image Processing 10 (2001) 266–277.
[13] H. Eschenauer, V. Kobelev, A. Schumacher, Bubble method for topology and shape optimization of structures, Structural and Multidisciplinary Optimization 8 (1994) 142–151.
[14] H. Eschenauer, N. Olhoff, Topology optimization of continuum structures: A review, Applied Mechanics Review 54 (2001) 331–390.
[15] M.I. Frecker, Recent advances in optimization of smart structures and actuators, Journal of Intelligent Material Systems and Structures 14 (2003) 207–216.
[16] E. Haber, A multilevel, level-set method for optimizing eigenvalues in shape design problems, Journal of Computational Physics 198 (2004) 518–534.
[17] L.L. Howell, Compliant Mechanisms, John Wiley & Sons Inc., New York, 2001.
[18] A.K. Jha, D.J. Inman, Optimal sizes and placements of piezoelectric actuators and sensors for an inflated torus, Journal of Intelligent Material Systems and Structures 14 (2003) 563–576.
[19] J. Juuti, K. Kordás, R. Lonnakko, V.-P. Moilanen, S. Leppävuori, Mechanically amplified large displacement piezoelectric actuators, Sensors and Actuators A 120 (2005) 225–231.

[48] M.Y. Wang, X.M. Wang, 'Color' level sets: a multiphase method for structural topology optimization with multiple materials, Computer Methods in Applied Mechanics and Engineering 193 (2004) 469–496.
[49] S.Y. Wang, K.M. Lim, B.C. Khoo, M.Y. Wang, An extended level set method for shape and topology optimization, Journal of Computational Physics 221 (2007) 395–421.
[50] P. Wei, M.Y. Wang, Piecewise constant level set method for structural topology optimization, International Journal for Numerical Methods in Engineering (2008), doi:10.1002/nme.2478.
[51] P. Wei, Level set methods for shape and topology optimization of structures, Ph.D. Thesis, The Chinese University of Hong Kong, 2007.
[52] J. Weickert, B.M. Romeny, M. Viergever, Efficient and reliable schemes for nonlinear diffusion filtering, IEEE Transaction on Image Processing 7 (1998) 398–410.
[53] Y.M. Xie, G.P. Steven, A simple evolution procedure for structural optimization, Computers & Structures 49 (1993) 885–896.
[54] H.K. Zhao, T.F. Chan, B. Merriman, S. Osher, A variational level set approach to multiphase motion, Journal of Computational Physics 127 (1996) 179–195.
[55] M. Zhou, G.I.N. Rozvany, The COC algorithm, Part II: topological, geometry and generalized shape optimization, Computer Methods in Applied Mechanics and Engineering 89 (1991) 197–224.